Empirical Gramian Based Controllability of Alternans in a Cardiac Map Model

Laura M Muñoz[1], Mark O Ampofo[1], Elizabeth M Cherry[2,1]

[1]Rochester Institute of Technology, Rochester, NY, USA
[2]Georgia Institute of Technology, Atlanta, GA, USA

Abstract

Electrical alternans, a beat-to-beat alternation in action potential duration, sometimes precedes the formation of dangerous cardiac arrhythmias. Controllability analysis answers questions about what types of interventions can suppress alternans or other unwanted phenomena in a dynamical model. Previously, we used a conventional linearization approach to determine controllability properties of the Qu, Shiferaw, and Weiss nonlinear map model of alternans dynamics. The model was of interest due to its ability to represent different drivers of alternans, including instabilities in voltage or calcium dynamics. Our computational methods had the disadvantage of requiring numerical evaluation of Jacobian matrices, a process that becomes computationally intensive for higher-dimensional systems. In the present study, we used a Jacobian-free "empirical" method to compute a measure of controllability based on minimum singular values of Gramian matrices and showed that empirical values matched closely with conventional ones. We compared the singular value measure with a modal controllability measure and demonstrated that the former predicts energy usage for certain scenarios, while the latter indicates strategies that lead to smaller sizes of alternans-suppressing perturbations.

1. Introduction

Electrical alternans is sometimes a precursor to complex abnormal heart rhythms, hence the search for alternans suppression methods remains an active area of research. To date, only a relatively small number of studies have investigated alternans from a control-theoretic perspective, for example by studying controllability, which is a model property that indicates whether a given suppression strategy is likely to succeed. Controllability helps answer questions about feasibility of strategies before a specific control algorithm, such as a formula that computes perturbations to the timing of electrical stimuli, is developed. In our recent work [1], we examined controllability of the Qu, Shiferaw, and Weiss (QSW) map model [2]. Our study was the first to evaluate effects of different drivers of alternans, such as voltage or calcium-related instabilities, on controllability. We compared control strategies that involved perturbing different dynamical variables and found that perturbing action potential duration, as opposed to adjusting calcium concentrations, appeared to be the best strategy regardless of alternans mechanism, according to a modal controllability measure. In the previous work, our controllability measures relied on Jacobian matrices, which are computationally cumbersome to estimate for higher-dimensional systems, and we restricted our analysis to a small number of control performance measures. To address these shortcomings, the present study offers the following novel contributions: (1) We used "empirical" methods, which avoid direct computation of Jacobian matrices, to estimate controllability Gramian matrices for the QSW model; (2) We compared two controllability measures with an extended set of performance indicators, which help explain cases in which the controllability measures favored different strategies.

2. Methods

The QSW model [2] has the form $X_{k+1} = f(X_k)$. The state vector is $X_k = [a_k\ b_k\ l_k]^T \in \mathbb{R}^n$, where a_k is cellular action potential duration (APD) (ms), b_k is the total intracellular calcium concentration CaTot (μM), l_k is the sarcoplasmic reticulum (SR) calcium load CaSR (μM), k is the stimulus index, T is the stimulus period (ms), and $n = 3$. Two configurations of model parameters were considered, yielding alternans that was either (1) voltage-driven and electromechanically discordant (EMD), where short APDs coincided with large peak calcium, or (2) calcium-driven and electromechanically concordant (EMC), where short APDs coincided with small peak calcium. Choices of parameters were explained previously [1]. All calculations were performed using Matlab.

Fixed points (solutions to $X^* = f(X^*)$) were estimated with Matlab's `fsolve` function (trust-region dogleg method) for periods in the range $T = 80$ to 600 ms. State matrices $A_d = \partial f/\partial X|_{X*}$ were determined using central-difference numerical approximations of Jacobians. For deviational state vector $x_k = S(X_k - X^*)$, a linearized dynamical equation $x_{k+1} = Ax_k + Bu_k$ was formed by adding control input u via input matrix B. For each parameter configuration, we computed a diagonal nondimensionalizing matrix S, where the diagonal entries were reciprocals of components of X^* for $T = 600$ ms. State vectors and matrices were obtained from their dimensional counterparts (subscripted d) via $x = Sx_d$, $A = SA_dS^{-1}$, and $B = SB_d$. We examined three control strategies for suppressing alternans, represented by $B_j = B_{APD} = S[1\ 0\ 0]^T$, $B_{CaTot} = S[0\ 1\ 0]^T$, or $B_{CaSR} = S[0\ 0\ 1]^T$, where the j-th control strategy perturbed the j-th state variable directly. Fixed point X^* represents a normal or period-1 rhythm, but for sufficiently short periods, X^* becomes unstable and alternans is the predominant behavior, which manifests as one or more alternans eigenvalues of A exiting the unit circle in the complex plane as T is lowered. "Alternans eigenvalue" refers to any eigenvalue of A with negative real part, and dynamical modes associated with alternans eigenvalues contribute a beat-to-beat alternation to system state trajectories. A typical goal of many alternans control methods is to restore stability of X^*.

Controllability measures were used to predict which strategies would be able to suppress alternans more effectively. A system is controllable if for any arbitrary initial state and arbitrary final state there exists a finite sequence of inputs that will transfer initial to final state. A linear system is controllable if controllability matrix $P = [B \quad AB \quad A^2B \quad \cdots \quad A^{n-1}B]$ (or controllability Gramian $W = PP^T$) is nonsingular. If $\sigma_{min}(W)$, minimum singular value of W, is nonzero, then the system is controllable and strategy B can suppress alternans or other unwanted behavior [3,4]. To avoid computing A matrices, which becomes cumbersome for high-dimensional systems, others (e.g., [5, 6]) have suggested computing "empirical" Gramians: $\hat{W} = \mathcal{X}_p\mathcal{X}_p^T/\rho^2$. Columns of $\mathcal{X}_p = [x_0\ x_1\ \ldots\ x_{q-1}]$ are sequential deviational states arising from simulating $X_{k+1} = f(X_k)$ from a perturbed initial state X_0 up to cycle index $q-1$. We chose $X_0 = X^* + \rho B_d$ with perturbation size ρ, where B_d is a column of the identity matrix indicating the control strategy. Next, $\hat{\sigma}_{min}$, the minimum singular value of $\hat{W}$, was determined for a range of values of ρ, using $q = 3$ steps, then compared with σ_{min} for different control strategies, period lengths, and alternans drivers. Mean absolute relative errors, averaged over all $N_T = 53$ periods, then over all $n = 3$ control strategies, were defined as:

$$\sigma_{err} = \frac{1}{nN_T}\sum_{j=1}^{n}\sum_{m=1}^{N_T}\left|\frac{\sigma_{min}(m,j) - \hat{\sigma}_{min}(m,j)}{\sigma_{min}(m,j)}\right|$$

We compared σ_{min} values to a modal controllability measure [7] defined as $|\cos\theta_{ij}| = |w_i^* \cdot B_j|/\|w_i^*\|\|B_j\|$, where θ is the controllability angle and w_i is the i^{th} left eigenvector of A. Larger $|\cos\theta_{ij}|$ indicates that the i-th eigenvalue of A is more strongly controllable through the j-th strategy. $|\cos\theta_{alt,j}|$ refers to controllability of the largest alternans eigenvalue, which is a measure of how well the j-th strategy can suppress alternans. In general, a strategy that yields stronger controllability (i.e., larger $\sigma_{\min}$ or $|\cos\theta|$) values is expected to produce smaller performance measures.

To aid in interpreting $\sigma_{\min}$ values, we examined $\max\|u_{min}\|$, which is an estimate of the worst-case minimum control energy over all initial condition directions. First, we computed $u_{min,l} = P^TW^{-1}(x_f - A^nx_{0,l})$ [3], which is the minimum-energy control input sequence (in the sense of minimizing $\Sigma_{k=0}^{k_f-1}u_k^2 = \|u\|_2^2$) needed to transfer $x_{0,l}$ to x_f in k_f steps [4]. Larger $\sigma_{\min}(W)$ is expected to lead to smaller energy expenditures. Here, it was assumed that $x_f = 0$ and initial conditions $x_{0,l} = Se_l$ were generated by drawing unit vectors e_l, $l \in \{1, 2, \ldots, 40\}$, from a zero-mean, unit-variance pseudorandom normal distribution. Performance measure $\max\|u_{\min}\| = \max_l\|u_{min,l}\|$ was calculated, with $\max\|Bu_{\min}\|$ defined similarly. Although u_{min} can be computed over a larger number of periods, $k_f = n = 3$ was used here for simplicity.

To produce another performance measure, we simulated the response of $x_{k+1} = Ax_k + Bu_k$ to state feedback algorithm $u = -Kx$, where linear quadratic regulator (LQR) control gain matrices $K = K_{LQR}$ were designed using Matlab's `dlqr` function, which yields gains K that minimize quadratic cost $J(K) = \sum_{k=0}^{\infty} x_k^TQx_k + u_k^TRu_k$. Here, diagonal penalty matrix Q and scalar R were chosen so that $R/\|Q\| = 0.125$, with remaining design details provided elsewhere [1]. A goal of LQR when X^* is unstable is to move eigenvalues back inside the unit circle in the complex plane; maximum moduli of $(A - BK_{LQR})$ eigenvalues resulting from our gain designs were 0.95 and 0.92 for the respective voltage- and calcium-driven cases. For each initial condition $x_{0,l}$, the system $x_{k+1} = Ax_k + Bu_k$ was simulated with control input $u_{LQR} = -K_{LQR}\ x$ for 20 periods, and nondimensional performance measure $\langle\|Bu_{LQR}\|\rangle$ was computed, where the average was taken over the 40 initial condition directions.

3. Results and Discussion

Examples of σ_{min} (solid lines) and $\hat{\sigma}_{min}$ (symbols $\times$, $\circ$, $+$) are displayed in the lower plots of Figures 1–2, for both the voltage- and calcium-driven cases. Larger σ_{min} indicates strategies that yield stronger controllability. APD bifurcation plots are included in the top panels to show the intervals of T over which alternans was the dominant long-term behavior. Plots were confined to $T \geq 150$ ms to exclude parts of the ranges over which 2:1 block occurs.

From the σ_{min} plots, it can be seen that for the three perturbation sizes included, empirical singular values matched closely with conventional values, though some discrepancies are visible for $\rho = 0.0001$ (marked with $\times$) in Figure 1 and for $\rho = 1$ (marked with $+$) in Figure 2.

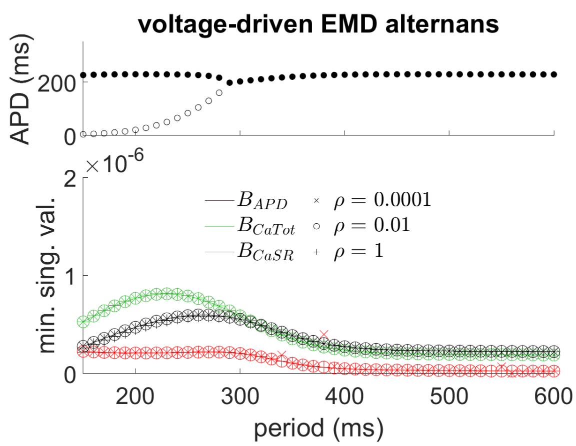

Figure 1: Top: APD vs. T bifurcation plot (showing alternans) arising from iterating QSW model for 1000 cycles at each period and plotting APDs from the final 10 periods. Alternating beats are shown with filled and open circles (graph adapted from [1]). Bottom: Minimum singular values of conventional Gramians W (solid lines) and empirical Gramians $\hat{W}$ ($\times$,$\circ$,$+$) for 3 different perturbation sizes (ρ), for voltage-driven EMD alternans. Color indicates control strategy.

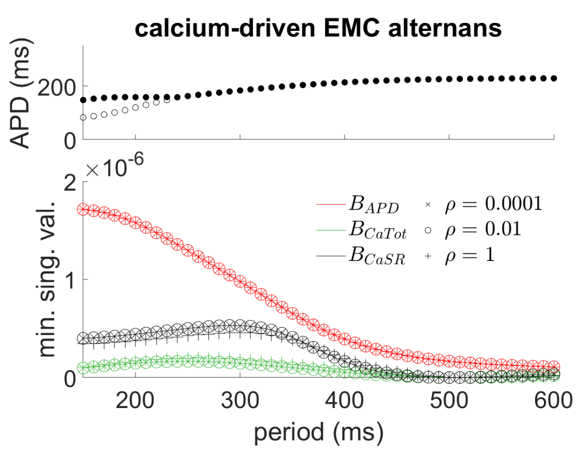

Figure 2: Top: APD bifurcation plot for calcium-driven EMC alternans. Bottom: Minimum singular values of conventional (solid lines) and empirical ($\times$,$\circ$,$+$) Gramians.

To quantify the accuracy of the minimum singular value estimates, mean absolute relative errors (σ_{err}) for several decades of ρ values are shown in Table 1. The ρ values that minimized σ_{err} differed depending on the parameter set. Nonetheless, there were various ρ values (such as 1×10^{-2}) that produced small errors for either alternans mechanism.

Examples of controllability measures $\sigma_{\min}(P)$, $\hat{\sigma}_{\min}(\hat{W})$, and $|\cos\theta_{alt}|$ are shown for three control strategies along with performance measures $\max\|u_{\min}\|$, $\max\|Bu_{\min}\|$, $\|BK_{LQR}\|$, and $\langle\|Bu_{LQR}\|\rangle$ for voltage- and calcium-driven alternans in Table 2. Periods of 230 and 150 ms were chosen since they approximately maximize APD alternans amplitudes while avoiding 2:1 block. Most quantities reported in the table were not shown previously, except for $\sigma_{\min}(P)$, $|\cos\theta_{alt}|$, and $\|BK_{LQR}\|$, which were given in [1] but are included here for comparison.

The table indicates that $\sigma^2_{\min}(P) = \hat{\sigma}_{\min}(\hat{W})$, which was expected due to properties of singular values; hence, the empirical $\hat{\sigma}$ values yield the same judgments about best control strategies as their conventional counterparts. From the perspective of the minimum singular values, the rankings of strategies from best to worst are B_{CaTot}, B_{CaSR}, and B_{APD} for the voltage-driven case and B_{APD}, B_{CaSR}, and B_{CaTot} for calcium-driven alternans. Modal controllability ($|\cos\theta_{alt}|$) rankings of strategies match those of $\hat{\sigma}_{\min}$ for calcium-driven alternans but not for the voltage-driven case. Specifically, modal controllability strongly favors suppressing alternans by adjusting the APD variable regardless of alternans mechanism, with a secondary preference for B_{CaSR} in the calcium-driven case.

Larger controllability values are expected to correlate with smaller performance measures, and the performance measures help to explain the sense in which any strategy is considered to be better or worse. Table 2 shows that $\sigma_{\min}$ predicted the ordering of $\max\|u_{\min}\|$ values as expected, while $|\cos\theta|$ predicted the ordering of overall perturbation sizes added to the system dynamics, specifically the $\|BK\|$, $\max\|Bu_{\min}\|$, and $\langle\|Bu_{LQR}\|\rangle$ measures. Hence, largest $\sigma_{\min}$ identifies the control strategy that yields the smallest of the worst-case minimum energy norms $\max\|u_{\min}\|$.

In the table, $\max\|Bu_{\min}\|$ exceeds $\langle\|Bu_{LQR}\|\rangle$ because the former is an aggressive control sequence that re-

Table 1: Mean absolute error (σ_{err}) of $\hat{\sigma}_{min}$ relative to σ_{min} for different alternans drivers and perturbation sizes, ρ. Smallest errors that were found are highlighted in blue.

ρ	Voltage-driven alt.	Calcium-driven alt.
1×10^{-5}	0.5262	0.0190
1×10^{-4}	0.1030	0.0018
1×10^{-3}	0.0133	0.0007
1×10^{-2}	0.0016	0.0062
1×10^{-1}	0.0015	0.0758
1×10^{0}	0.0144	2.1026
1×10^{1}	0.1657	45.7828

Table 2: Controllability values ($\sigma_{\min}$, $\hat{\sigma}_{\min}$, and $|\cos\theta|$) and performance measures for three control strategies (B_{APD}, B_{CaTot}, B_{CaSR}) for electromechanically discordant voltage-driven (mechanism: V) alternans at a period of 230 ms (rows 2–4) and electromechanically concordant calcium-driven (mechanism: Ca) alternans at a period of 150 ms (rows 5–7).

Mech.	Strategy (B)	$\sigma_{\min}(P)$	$\hat{\sigma}_{\min}(\hat{W})$	max$\|u_{\min}\|$	max$\|Bu_{\min}\|$	$\|\cos\theta_{alt}\|$	$\|BK_{LQR}\|$	$\langle\|Bu_{LQR}\|\rangle$
V	B_{APD}	0.0005	2.12×10^{-7}	27.4201	0.1201	0.9997	9.81×10^{-1}	0.0030
	B_{CaTot}	0.0009	8.13×10^{-7}	19.6495	0.2819	0.0219	$4.48\times10^{+1}$	0.1229
	B_{CaSR}	0.0007	5.58×10^{-7}	22.4201	0.6570	0.0094	$1.04\times10^{+2}$	0.2907
Ca	B_{APD}	0.0013	1.71×10^{-6}	7.2572	0.0317	0.8522	4.30×10^{-1}	0.0023
	B_{CaTot}	0.0003	9.65×10^{-8}	20.2061	0.1766	0.1238	$2.96\times10^{+0}$	0.0202
	B_{CaSR}	0.0006	4.00×10^{-7}	10.2019	0.1294	0.5084	7.22×10^{-1}	0.0053

turns the state to the origin in 3 periods, compared with LQR, which moves x_k toward the origin more gradually. Since LQR and other state feedback input sequences can be calculated independently of any knowledge of initial and final states, they are typically considered a more practical method of controlling a system compared with the u_{min} approach. Furthermore, unlike LQR, u_{min} does not necessarily stabilize fixed points.

We chose to examine multiple controllability measures since it is not yet certain which aspects of control performance should receive highest priority, though many other measures could have been considered besides those shown. Considering the greater practicality of LQR and the nondimensionality of quantities like $\|BK\|$, it appears that rankings of strategies based on $|\cos\theta|$ should be favored over those of $\sigma_{\min}$ in cases of disagreement, but the latter is still a well-known measure that can offer insights into possibilities for energy usage. A limitation is that other choices of nondimensionalizing transformations could yield different orderings of either set of controllability rankings, though re-orderings are more likely for strategies that are already close in value in the table.

4. Conclusions

In this study, we computed controllability Gramians for the QSW alternans model using an "empirical" or Jacobian-free method and showed that the resulting minimum singular values were similar to conventional values. We compared the singular value controllability measure with a modal measure to determine best control strategies for suppressing alternans. The modal measure favored perturbing APD, as opposed to calcium-related variables, as the best strategy for both the voltage- and calcium-driven alternans cases. Modal controllability aligned with measures of control perturbation size, though the singular value measure gave information on energy usage in a type of worst-of-the-best case scenario. Our work is part of a broader effort to provide computationally efficient tools for assessing alternans controllability, which could facilitate decisions about control strategies and electrode placements when applied to spatially distributed models of tissue.

Acknowledgments

This work was supported, in part, by the National Science Foundation under Grant Nos. CNS-1446312 and CNS-2028677.

References

[1] Muñoz LM, Ampofo MO, Cherry EM. Controllability of voltage- and calcium-driven cardiac alternans in a map model. Chaos An Interdisciplinary Journal of Nonlinear Science February 2021;31(2):023139. ISSN 1054-1500, 1089-7682.

[2] Qu Z, Shiferaw Y, Weiss JN. Nonlinear dynamics of cardiac excitation-contraction coupling: An iterated map study. Physical Review E January 2007;75(1):011927. ISSN 1539-3755, 1550-2376.

[3] Brogan WL. Modern Control Theory. 3rd ed edition. Englewood Cliffs, N.J: Prentice Hall, 1991. ISBN 978-0-13-589763-8.

[4] Bryson AE, Ho YC. Applied Optimal Control: Optimization, Estimation, and Control. Rev. print edition. New York: Taylor & Francis, 1975. ISBN 978-0-89116-228-5.

[5] Lall S, Marsden JE, Glavaški S. Empirical model reduction of controlled nonlinear systems. IFAC Proceedings Volumes July 1999;32(2):2598–2603. ISSN 14746670.

[6] Tu JH, Rowley CW. An improved algorithm for balanced POD through an analytic treatment of impulse response tails. Journal of Computational Physics June 2012;231(16):5317–5333. ISSN 00219991.

[7] Hamdan AMA, Nayfeh AH. Measures of modal controllability and observability for first- and second-order linear systems. Journal of Guidance Control and Dynamics 1989; 12(3):421–428.

Address for correspondence:

Laura Muñoz
Rochester Institute of Technology
85 Lomb Memorial Drive, Rochester, NY, USA, 14623
laura.m.munoz@gmail.com